Finite Difference Time Domain Analysis of Two Dimensional Photonic Bandgap Devices

تحليل أجهزة البلورات الفوتونية ثنائية البعد باستخدام طريقة الفروق المحدودة في النطاق الزمني

Nihal F. Areed, Salah S. A. Obayya, and Hamdi A. El-Mikati

Department of Electronics and Electrical Communications Engineering, Mansoura University, Mansoura, Egypt.

الملخص: في هذا البحث تستخدم طريقة الفروق المحدودة في النطاق الزمني لتحليل انتشار النبضات المستقطبة كهربيا و عرضيا في البلورات الفوتونية. و تتم حساب الفجوة في المدى الترددي لنوعين من البلورات الفوتونية ثنائية البعد بثلاث طرق و هي حساب منحنى التشتت و منحنى الانتشار و طريقة عمل فجوة خطية. بعد ذلك تم تحليل نوعين من أجهزة البلورات الفوتونية و دراسة خصائصها.

Abstract: A Finite Difference Time Domain (FDTD) analysis has been effectively applied to investigate the transmission of the transverse electric polarized pulses in photonic crystals arrangements. The photonic bandgap of 2-D photonic crystal with square and veins lattices has been calculated using three methods Band structure, transmission diagram and defected structures, and comparison with published results are done and excellent agreement are obtained. Moreover, two different photonic crystal devices are analyzed

Index Terms: Photonic Crystal [PC], Finite Difference Time Domain (FDTD), Photonic Bandgap (PBG).

I. Introduction

Photonic crystals (PCs) are periodic dielectric or metallo-dielectric (nano)structures that are designed to affect the propagation of electromagnetic waves (EM) in the same way as the periodic potential in a semiconductor crystal affects the electron motion by defining allowed and forbidden electronic energy bands. The absence of allowed propagating EM modes inside the structures, in a range of wavelengths called a photonic band gap, gives rise to distinct optical phenomena such as inhibition of spontaneous emission, high-reflecting omni-directional mirrors and low-loss-wave guiding among others[1].

According to the number of directions in which dielectric materials exhibit periodicity, one, two, or three dimensional photonic crystal structures are possible [2].

A two dimensional system exhibits most of the important characteristics of photonic crystal structures. This type has a periodic geometry in two directions and homogeneous in the third. There are many types of two dimensional photonic crystal systems such as square , triangular, honeycomb and veins lattices [3-4].

Researches over the last decade have generated a wide range of rigorous numerical algorithms for modeling photonic crystal structures, such as plane-wave expansion (PWE) and finite element methods [5]. These versatile algorithms have been applied with success to study issues such as dispersion relation and propagation characteristics for PC structures.

In this paper, Finite Difference Time Domain (FDTD) Technique has been utilized to calculate the photonic bandgap of 2D PCs with different lattice arrangements and to analyze two different types of photonic bandgap devices.

This paper is organized as follows Following this introduction, a brief mathematical treatment of FDTD method is given in section II Methods of calculating PBG are given in section III. Section IV detailed the results and their physical explanation. Finally, some conclusions are presented in section V.

II. Formulation

A- Basic Equations

In a two-dimensional case, the fields can be decoupled into two transversely polarized modes, namely the E polarization (E_z, H_x, and H_y) and the H polarization (H_z, E_x, and E_y). Yee's mesh is widely used in the FDTD analysis [6] Here, Yee's two dimensional mesh in Finite Difference Time Domain solver is used. The unit

Accepted April 5, 2007

Yee cell of the two-dimensional mesh for E polarization case is illustrated in Fig.1.

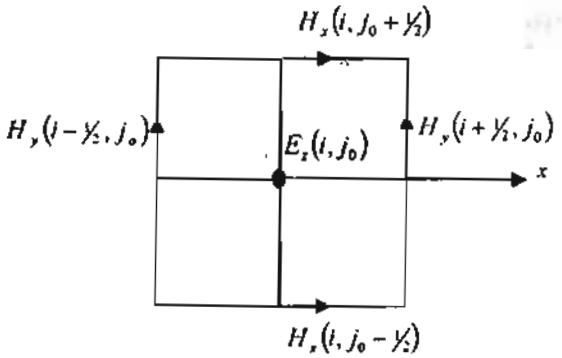

Fig. 1. The unit Yee cell of the two-dimensional FDTD mesh for E polarization case[6].

The continuity conditions are automatically satisfied since; all the transverse field components are tangential to the unit cell boundaries. The following 2-D FDTD time stepping formulas constitute the discretization (in space and time) of Maxwell's equations on a discrete two-dimensional mesh in a Cartesian x y coordinate system for E polarization case:

$$H_x\Big|_{i,j}^{n+\frac{1}{2}} = H_x\Big|_{i,j}^{n-\frac{1}{2}} - \frac{\Delta t}{\mu_{i,j}}\left[\frac{E_z\Big|_{i,j+1}^{n} - E_z\Big|_{i,j}^{n}}{\Delta y}\right], \quad (1\text{-a})$$

$$H_y\Big|_{i,j}^{n+\frac{1}{2}} = H_y\Big|_{i,j}^{n-\frac{1}{2}} + \frac{\Delta t}{\mu_{i,j}}\left[\frac{E_z\Big|_{i+1,j}^{n} - E_z\Big|_{i,j}^{n}}{\Delta x}\right], \quad (1\text{-b})$$

$$E_z\Big|_{i,j}^{n+1} = \frac{\varepsilon_{i,j} - \sigma_{i,j}\Delta t/2}{\varepsilon_{i,j} + \sigma_{i,j}\Delta t/2} E_z\Big|_{i,j}^{n} + \frac{\Delta t}{\varepsilon_{i,j} + \sigma_{i,j}\Delta t/2}\left[\frac{H_y\Big|_{i,j}^{n+1/2} - H_y\Big|_{i-1,j}^{n+1/2}}{\Delta x} - \frac{H_x\Big|_{i,j}^{n+1/2} - H_x\Big|_{i,j-1}^{n+1/2}}{\Delta y}\right], \quad (1\text{-c})$$

and for H polarization case :

$$E_x\Big|_{i,j}^{n+1} = \frac{\varepsilon_{i,j} - \sigma_{i,j}\Delta t/2}{\varepsilon_{i,j} + \sigma_{i,j}\Delta t/2} E_x\Big|_{i,j}^{n} + \frac{\Delta t}{\varepsilon_{i,j} + \sigma_{i,j}\Delta t/2}\left[\frac{H_z\Big|_{i,j}^{n+1/2} - H_z\Big|_{i,j-1}^{n+1/2}}{\Delta y}\right], \quad (2\text{-a})$$

$$E_y\Big|_{i,j}^{n+1} = \frac{\varepsilon_{i,j} - \sigma_{i,j}\Delta t/2}{\varepsilon_{i,j} + \sigma_{i,j}\Delta t/2} E_y\Big|_{i,j}^{n} - \frac{\Delta t}{\varepsilon_{i,j} + \sigma_{i,j}\Delta t/2}\left[\frac{H_z\Big|_{i,j}^{n+1/2} - H_z\Big|_{i-1,j}^{n+1/2}}{\Delta x}\right], \quad (2\text{-b})$$

$$H_z\Big|_{i,j}^{n+1/2} = H_z\Big|_{i,j}^{n-1/2} - \frac{\Delta t}{\mu_{i,j}}\left[\frac{E_y\Big|_{i+1,j}^{n} - E_y\Big|_{i,j}^{n}}{\Delta x} - \frac{E_x\Big|_{i,j+1}^{n} - E_x\Big|_{i,j}^{n}}{\Delta y}\right] \quad (2\text{-c})$$

where superscript n indicates the discrete time step, subscripts i and j indicate the position of a grid point in the x, and y directions, respectively. Δt is the time increment, and Δx, and Δy are the space increments between two neighboring grid points along the x and y directions, respectively ω is the angular frequency, μ , ε and σ are the permeability, the permittivity and the conductivity of the medium considered.

C- Stability Condition

For two-dimensional FDTD time-stepping formulas, the stability conditions for an orthogonal case is [6]

$$\Delta t \le \frac{1}{c\sqrt{(\Delta x)^{-2} + (\Delta y)^{-2}}} \quad (3)$$

III. Methods of Calculating PBG

A. Band Structure

When calculating the band structures of photonic crystals, one naturally chooses a unit cell of lattice as the finite computation domain (Brillouin zone), and uses the periodic boundary condition, which satisfies the Bloch theory [3] as shown in Fig. 2. Therefore, we have the following simple boundary conditions for updating the fields,

$$\vec{E}(\vec{r} + \vec{L}) = e^{i\beta L}\vec{E}(\vec{r}), \qquad \vec{H}(\vec{r} + \vec{L}) = e^{i\beta L}\vec{H}(\vec{r}). \quad (4)$$

where L is the lattice vector.

In FDTD method, all the fields are obtained in the time domain. However, the dispersion relation (the band structures, guided modes, etc) of a photonic crystal is a relation between the frequency and the wave vector Therefore, we need to perform a Fourier transform,

$$u(\omega) = \int_{-\infty}^{+\infty} u(t) e^{i\omega t} dt , \quad (5)$$

where u is one of the field components. Unfortunately, the exact Fourier transform cannot be obtained since the information about u(t) for t<0 is not available in our computation However, one is not interested in the exact spectral shape of Fourier transform but the peaks of the spectral distribution, which correspond to the locations of the eigen frequencies. Therefore, one can use the following transformation to obtain the spectrum,

$$u(\omega) = \int_0^{N_t} u(t)\, e^{-i\omega t}\, dt \qquad (6)$$

$$\approx \sum_{n=0}^{N_t} u(n\Delta t)\, e^{-in\omega\Delta t}\, \Delta t,$$

where N_t is the total number of time steps. The peaks of the function u(ω) are located at the same places as the peaks in the Fourier transform of u(t), and these peaks become higher (more obvious) as N_t increases.

One should subtract the static component from the fields so that their time average is zero. Also, it is not always necessary to calculate the above transformation at all the discretization points in the unit cell of lattice (the computation domain). One may choose 100 points randomly and then sum up the spectral amplitudes at all these points,

$$u(\omega) = \sum_{i,j} \left| \sum_{n=0}^{N_t} \left(u_{i,j}(n\Delta t) - \frac{1}{n} \sum_{m=0}^{n} u_{i,j}(m\Delta t) \right) e^{-in\omega\Delta t} \Delta t \right|. \quad (7)$$

where (i,j) indicates the 100 randomly chosen points. The peaks of the spectral function U(i,j) indicate the locations of the eigen frequencies ω.

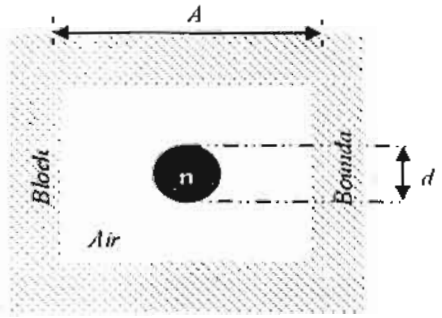

Fig.2. One Unit Cell of square lattice Photonic crystal structure

B. Transmission Diagram

In this method, we suppose that a Gaussian pulse propagates normally (normal incidence) to the 2-D photonic crystal. A perfectly matched layer (PML) with the following impedance matching condition [7] is applied to bound the computational window. In the PML, the electric or magnetic field components are split into two subcomponents (e.g., $E_z = E_{zx} + E_{zy}$) with the possibility of assigning losses to the individual split field components.

$$\frac{\sigma_e}{\varepsilon_o n^2} = \frac{\sigma_m}{\mu_o} \qquad (8)$$

where σ_e and σ_m are the electric and magnetic conductivities of the PML, respectively, and n is the refractive index of the adjacent computing domain, which means that the wave impedance of a PML medium exactly equals to that of the adjacent medium in the computing window regardless of the angle of propagation.

The transmission is computed by comparing incident and transmitted energy and is given by the following relation [6]

$$T_f(\omega_f) = \frac{P(y_{trans}, \omega_f)}{P(y_{inc}, \omega_f)}, \qquad (9)$$

where, y_{inc} is a value of y at the very beginning of the domain and y_{trans} at the very end.

There may be numerical problems computing transmission with (9), for example unexpected reflections. An alternative way is to use a reference structure. Then we compute the power flows $P^{ref}(y_{trans})$ and $P^{ref}(y_{inc})$ for a structure where the subject of interest does not appear in the specified problem, for example a waveguide without holes. Then we do the computations once again, with the interesting subject appearing. Now, the transmission becomes:

$$T_f(\omega_f) = \frac{P(y_{trans}, \omega_f)}{P^{ref}(y_{trans}, \omega_f)}. \qquad (10)$$

This is the fraction of energy that passes through an area at $y = y_{trans}$ with and without a specific subject.

The diagram of transmission of this crystal gives the presence of band gaps if exist.

This method also is used for calculating the propagation characteristics of two types of photonic bandgap devices: filter and splitter.

C. Defected Structure

This method is used for ensuring the existence of PBG through calculating the electric field pattern. If one introduces a line defect (i.e., a waveguide) into a photonic crystal which has a photonic band gap, one can guide light (whose frequencies are within the photonic band gap) from one location to another since light has nowhere else to go.

IV. Numerical results

First, we used the three numerical methods outlined above to calculate the band gap of a two-dimensional square lattice of dielectric rods in air, in which the dielectric 'atoms' are isolated. The radius of the rod is R=0.18a (A is the lattice constant A=0.58 μm) [8]. The dielectric constant of the rods is ε_r=3.4 as inset in Fig. 3.a. Figure 3.b shows the band structures of the photonic crystal for E polarizations case, In this case, only, one cell has been discretized with a uniform mesh [Δx × Δy] are [0.0145μm × 0.0145μm], the time step Δt is 0.023586 *fs* and the simulation time is 500 *fs*. On a PC (Pantium IV, 3.2GHz, 2GB RAM), the whole simulation period took around 20 min. Also, the transmission power spectrum is calculated in Fig.4.b. While, in this case, this structure has been discretized with a uniform mesh where the computational window sizes [x × y] are [11.6μm × 5.8μm], the time step Δt is 0.0171002 *fs* and the simulation time is 3000 *fs*. The PML layers are assumed to be 50 layers. On a PC (Pantium IV, 3.2GHz, 2GB RAM), the whole simulation period took around 45 min. One can see from these Figures that there is only large band gap for the E polarization around the normalized frequency 0.34. Moreover, this is obvious from the electric field pattern when an electromagnetic wave propagates through a photonic crystal waveguide with essentially a 100% transmission when the wavelength equals 1.5 μm; however, there is no propagation for wavelength equals 1.16μm as shown in Fig. 5.

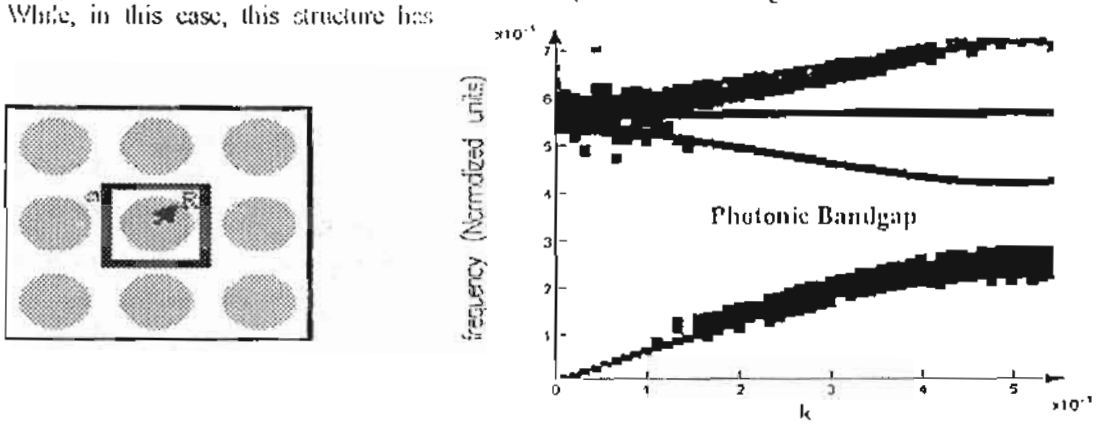

Fig. 3. Square lattice of dielectric rods in air: (a) Details of the structure R=0.18A , ε_r=3.4, (b) Dispersion diagram for E polarization case.

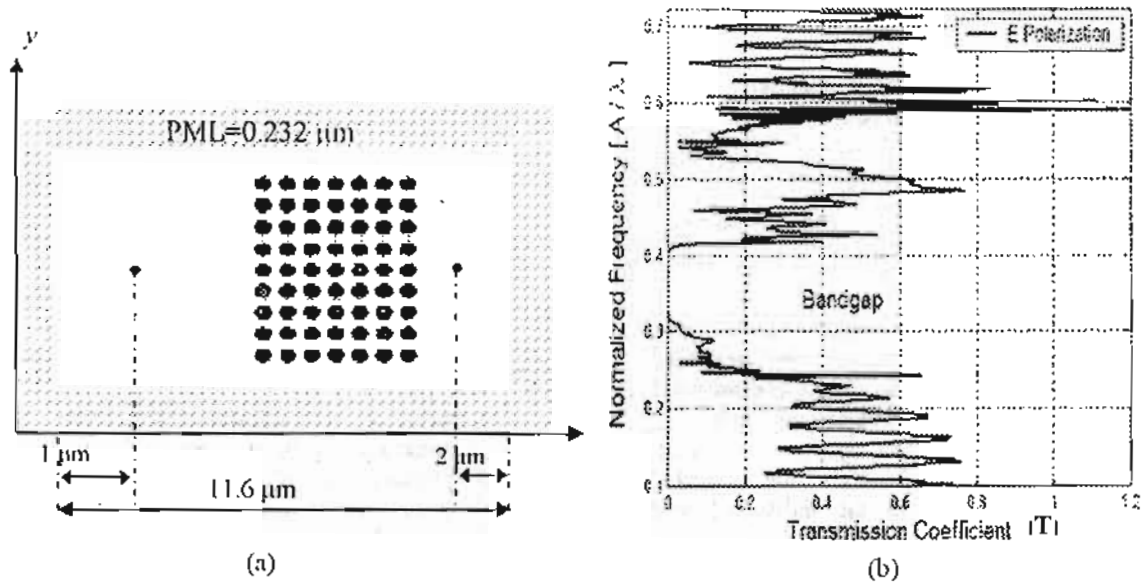

Fig. 4. Square lattice of dielectric rods in air: (a) Details of the structure, (b) Transmission diagram.

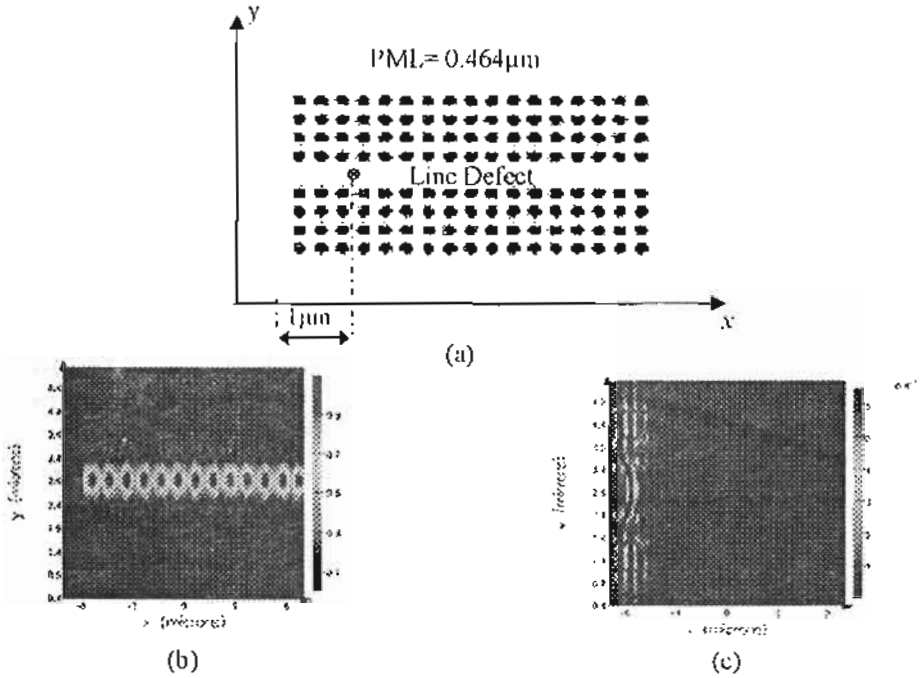

Fig. 5. Defected structures (a) $\lambda=1.5um$, (b) $\lambda=1.16$um

The above results help to calculate the Bloch modes of the first Brillouin zone.

As shown in Fig. 6, the Bloch modes are calculated for 1.309 μm and 1.736526 μm, respectively

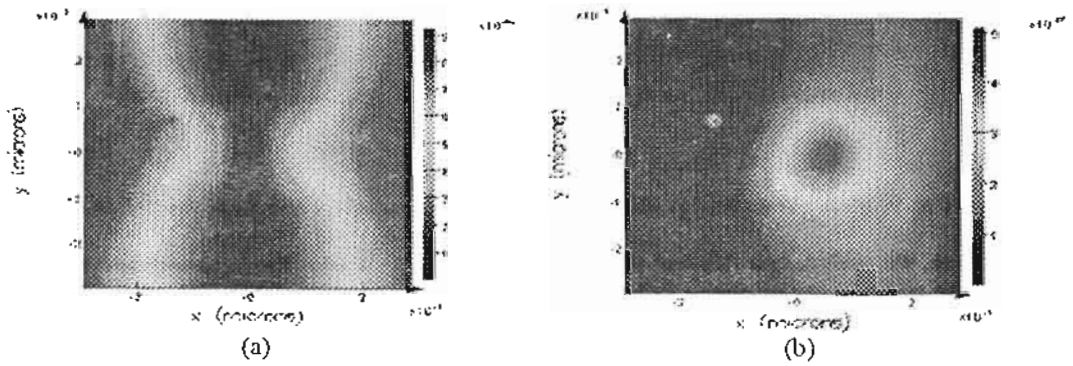

Fig. 6. Bloch modes (a) λ_1= 1.309 μm , (b) λ_2=1.736526 μm.

Next, consider another two-dimensional photonic crystal, a square lattice of dielectric veins, in which the dielectric 'atoms' are connected as inset in Fig. 7. Figure 8 shows the band structure and transmission diagram for H polarization case with half vein width $d=0.120a$ [3]. From Fig. 8, one can see that there is a band gap for the H polarization around the frequency 0.350 ($\omega a/2\ \pi c$). Therefore, it appears that E polarization band gaps are favored in a lattice of isolated high- ε regions, and H polarization band gaps are favored in a connected lattice. This is a rule of thumb for photonic band gaps. Furthermore, this is obvious from the electric field pattern when an electromagnetic wave propagates through a defected photonic crystal structure as demonstrated in Fig. 9.

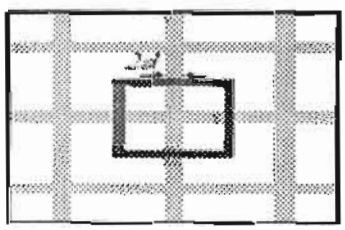

Fig. 7 Square lattice of dielectric veins in air. The half vein width is $d=0.120a$. The dielectric constant of the veins is $\varepsilon=11.4$.

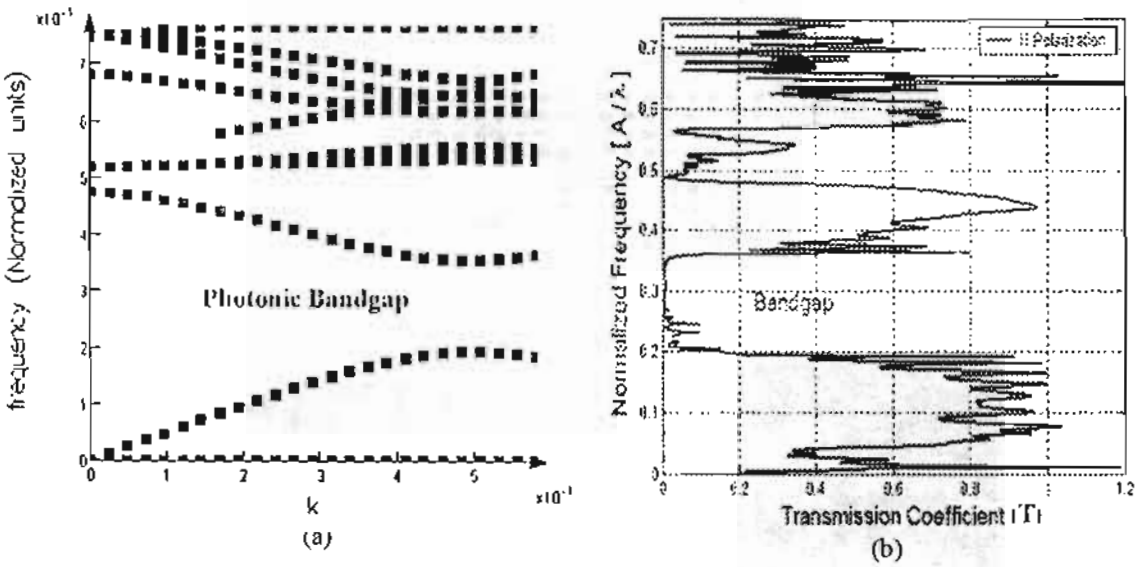

Fig. 8. Square lattice of dielectric veins in air: (a) Dispersion relation for H polarization, (b) Transmission diagram.

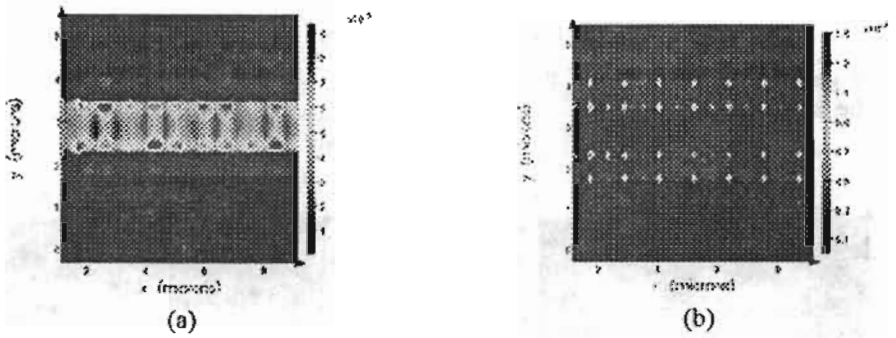

Fig. 9. Steady state field profile of defected structures at: (a) $\lambda=1.5um$, (b) $\lambda=1.16$um.

Now, we analyze two different photonic crystal circuit components as shown in Figs 10-16 and simulate those propagation characteristics. For all examples presented in connection with photonic crystal circuits in this subsection, the circuits are held in the above analyzed square lattice shown in Fig. 3.a and the input Gaussian pulse are the same at central wavelength 1.55 μm and fed at point *P1*.

First, we consider different numbers of micro-cavities coupled to straight waveguides as shown in Fig. 10.a and Fig. 11. The computational window sizes [x × y] are [53.94μm × 6.85125μm], the time step Δt is 0.0641259 *fs* and the simulation time is 5000 *fs*. The PML layers are assumed to be 20 layers. On a PC (Pantium IV, 3.2GHz, 1GB RAM), the whole simulation period took around 30 min.

From the transmission characteristics shown in Fig. 10.b, it is clear that, with the increase of the number of circular rods in the center of the PC waveguide, there is a decrease of the amount of the transmitted power to at point *P2* in the structure shown in Fig. 10.a.

On the other hand, inserting a single cavity can produce an optical filter with a sharp transmission resonance. Fig. 12.a shows that , the single cavity should be held only in the centre of the circular rods to achieve filter with high sharp transmission resonance. The results obtained by the finite element method are presented in reference [8] and excellent agreement is obtained. Varying the width of the single cavity will changes the frequency resonant point as inset in Fig. 12.b. Moreover, Fig. 13 shows that, increasing the number of micro-cavities will increase the bandwidth of the PC filter.

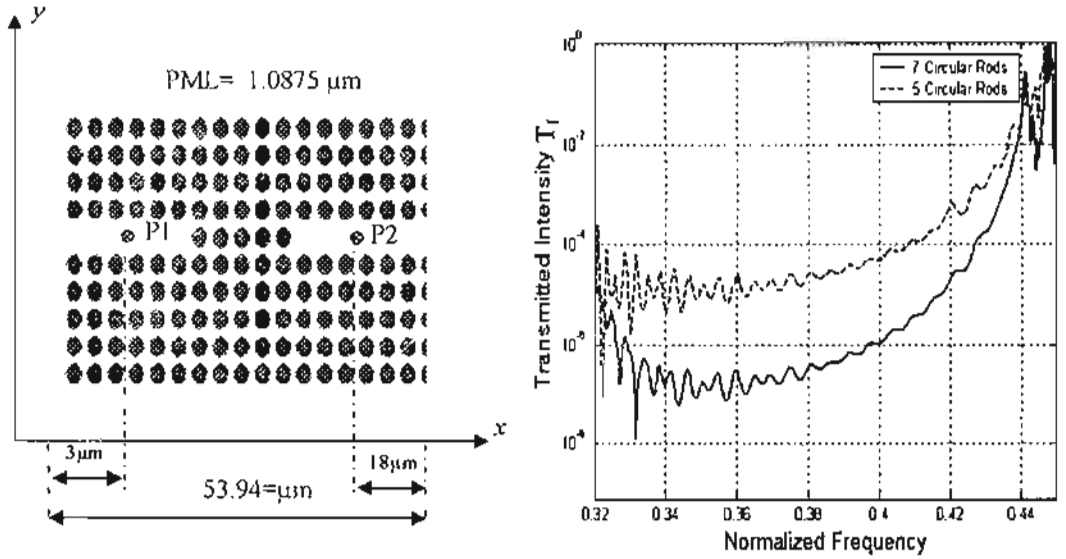

(a) (b)

Fig. 10. Square lattice of dielectric rods in air with line defect: (a) Structure geometry, (b) Transmission diagram.

(a) (b) (c)

Fig. 11. Photonic crystal filter with: (a) Single cavity , (b) Double cavities, (c) Terrible cavities.

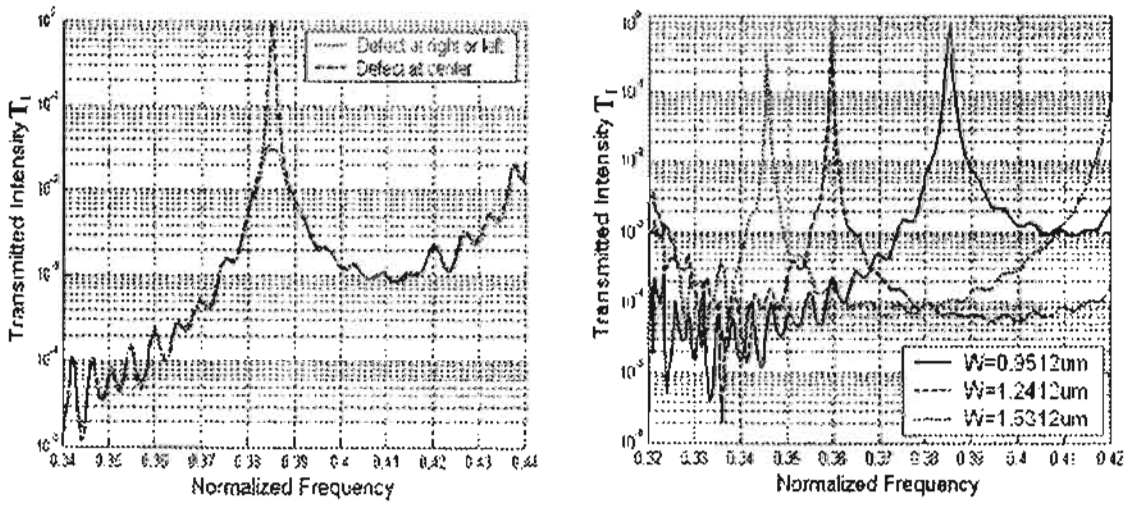

(a) (b)

Fig. 12. Propagation Characteristics for PC Filter with: (a) Single cavity filter, (b) Propagation characteristics for PC filter with single cavity versus different defect widths.

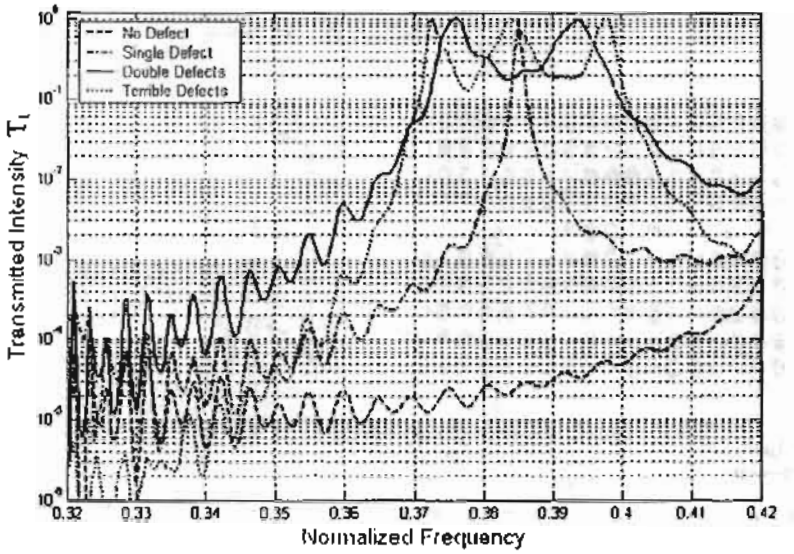

Fig. 13. Comparison between PC filters with different number of cavities.

Finally, Fig. 14.a shows a T- branch PC splitter. The computational window sizes [x × y] are [53.94μm × 11.471μm], the time step Δt is 0.0645129 *fs* and the simulation time is 1800*fs*. The PML layers are assumed to be 20 layers. On a PC (Pantium IV, 3.2GHz, 1GB RAM), the whole simulation period took around one hour. From the calculated propagation characteristics shown in Fig. 14.b, the high transmission is observed at normalized frequency ranges from 0.386 to 0.403. Also the two ports of the PC splitter have obtained approximately the same amount of the transmitted intensity over the same considered frequency range. On the other hand, the transmission properties of splitters shown in Figs. 15 and 16 are also high but, each port has obtained a different amount of transmitted intensity than the other for specific values of frequencies. This device could be used for designing a multiplexer consisting of such a splitter followed by a filter in each arm tuned to the corresponding frequency.

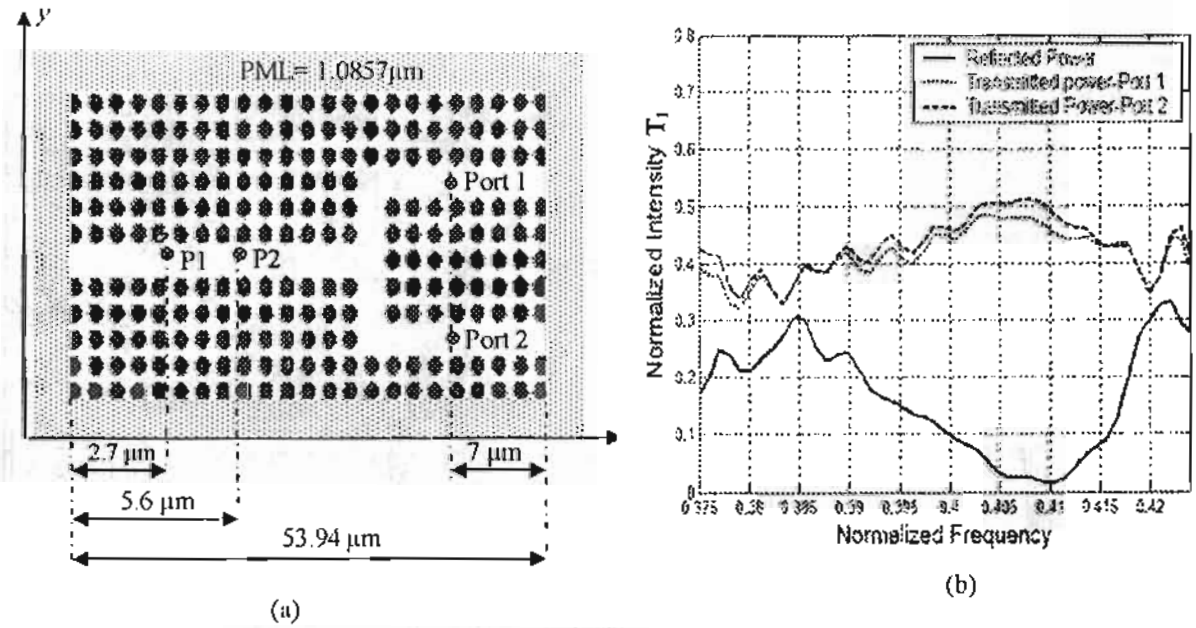

Fig. 14. PC splitter of dielectric rods in air: (a) Structure geometry, (b) Propagation characteristics.

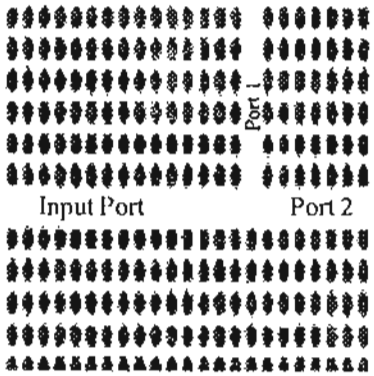

(a)

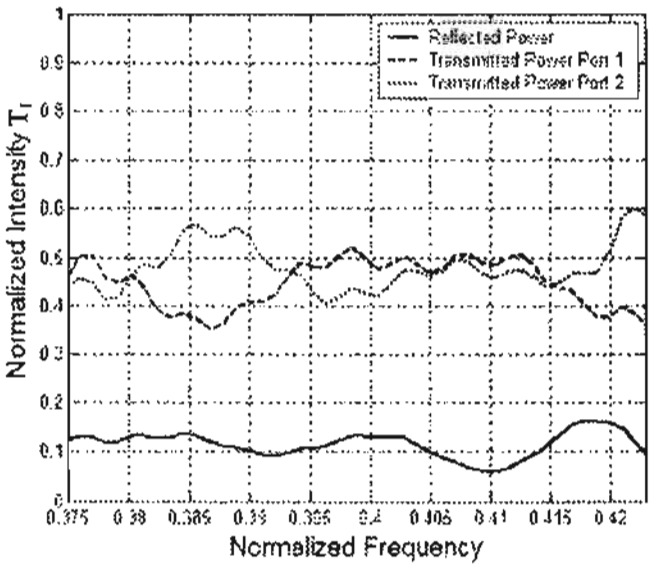

(b)

Fig. 15. PC splitter of dielectric rods in air: (a) Structure geometry, (b) Propagation characteristics.

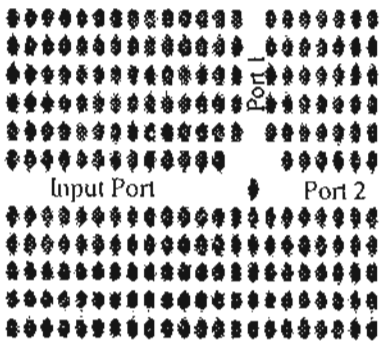

(a)

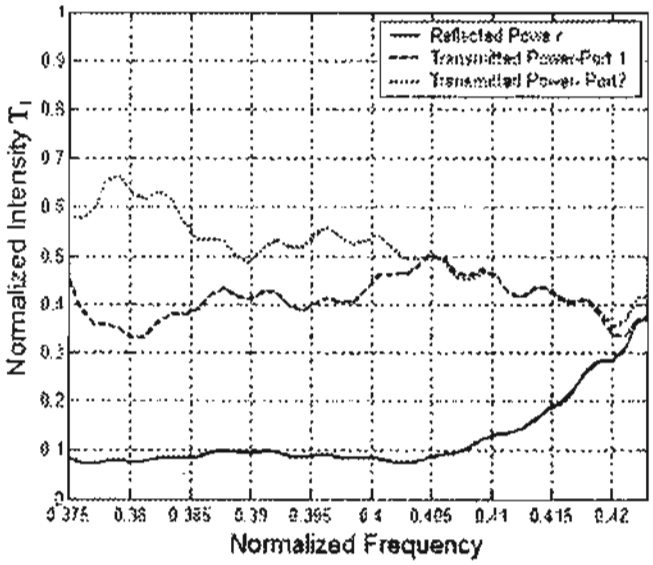

(b)

Fig. 16. PC splitter of dielectric rods in air: (a) Structure geometry, (b) Propagation characteristics.

V. Conclusion

Finite difference Time Domain algorithm incorporated with Bloch periodic or perfectly matched layer absorbing boundary condition is formulated for the calculating the band gap of different lattices of 2-D photonic crystal structures. To validate the program, comparison with the finite element method in frequency domain is obtained and showed an excellent agreement. Furthermore, two different photonic crystal circuit components were simulated and their fascinating properties were presented.

VI. References and Web Links

1. http://www.azonano.com/Details.asp?ArticleID=1256
2. http://www.public.iastate.edu/~cmpexp/groups/ho/pbg.html
3. Min Qiu, Computational methods for the analysis and design of Photonic bandgap structures, Ph. D., Royal Institute of Technology, Stockholm, 2000.
4. Joen I. Kim , Analysis and applications of microstructure and holey optical fibers, Ph. D., Virginia State University, 10 Sept. 2003.
5. J. M. Lourtioz, H. Benisty V. Berger, J. M. Gerard D. Maystre, and A. Techelonkov, Photonic Crystals towards Nanoscale Photonic Device, Springer Verlag Berlin Heidelberg, 2005.
6. Tommy Sundstrom, Analysis of Photonic Crystal Waveguides by the use of FDTD with Regularization, KTH Numerical Analysis and Computer Science, Stockholm, 2004.
7. Chin-Ping Yu and Hung-Chun Chang, "Yee-mesh-based finite difference eigenmode solver with PML absorbing boundary conditions for optical waveguides and photonic crystal fibers," Opt. Express, Vol. 12, No. 25, pp. 6165-6177, 13 December 2004.
8. Masanori Koshiba, Yasuhide Tsuji, Masafumi Hikari, "Time Domain Beam Propagation Method and Its Application to Photonic Crystal Circuits," IEEE Journal of Lightwave Technol., Vol. 18, No. 1, pp. 102-110, January 2000.